Detection of pathological changes in the architectonics of polycrystalline blood films using laser-induced polarization interferometry

Kvasniuk D.[1], Trifonyuk L.[2], Strashkevich A.[3], Kozan N.[1],Ushenko V.[4], Dunaiev O.[4], Kryvetskyi V.[4], Oliinyk I.[1], Kurek E.I.[4], Tkachuk V.I.[4]
[1] Bukovinian State Medical University, Chernivtsi, Ukraine
[2] Rivne State Medical Hospital, Rivne, Ukraine
[3]The Institute of Traumatology and Orthopedics by NAMS of Ukraine, Kyiv, Ukraine
[4]Chernivtsi National University, Chernivtsi, Ukraine

ABSTRACT

The paper presents the results of the possibility of a polarization-interference approach to the analysis of microscopic images polycrystalline blood films of patients of benign and malignant prostate tumours with different degrees of differentiation. Measurements and analysis of maps and histograms of the distribution of the local contrast value of polarization-interference distributions of microscopic images of polycrystalline blood films of patients . Determination of the relationship between the statistical moments of the 1st - 4th orders characterizing the distributions of the local contrast value of the polarization-interference distributions of microscopic images of polycrystalline blood films of patients. Determination of statistical criteria for polarization-interference diagnosis of histological sections of biopsy of adenoma and adenocarcinoma with varying degrees of differentiation. Determination of sensitivity, specificity, accuracy of the polarization interferometry method for differential diagnosis of polycrystalline blood films of patients of adenoma and adenocarcinoma with varying degrees of differentiation.

Keywords: laser, polarization, interference, contrast, image, statistical moments of the 1st - 4th orders, blood, adenoma, adenocarcinoma, sensitivity, specificity, accuracy

1. STRUCTURAL-LOGICAL AND OPTICAL SCHEME OF POLARIZATION INTERFEROMETRY OF MICROSCOPIC IMAGES OF BIOLOGICAL LAYERS

In fig. 1 shows the structural and logical diagram and design of the method of polarization [1-7] interferometry [8-20] of microscopic images of histological sections of biopsy of prostate tumours.

1	Optical probing source	Gas helium-neon laser; Wavelength 0.6328 μm
2	Block for forming the spatial structure of the optical probe	Optical collimator for forming a parallel laser beam with a cross section of 5 mm
3	Multichannel block for the formation of the polarization structure of the optical probe	System of formation of linear ($0^0;90^0;45^0$) and right-circular polarization (linear polarizer (Achromatic True Zero-Order Waveplate) - quarter-wave plate (B + W Kaesemann XS-Pro Polarizer MRC Nano)).
4	Object block	Microscopic coordinate node
5	Formation block of microscopic image	Polarizing micro lens (Nikon CFI Achromat P, working distance – 30mm, focal distance - 50mm, NA – 0.1, magnification – 4x)
6	Multichannel polarization filtering block	Transmission system of linearly ($0^0;90^0;45^0;135^0$), right- and left-circularly polarized components

Fifteenth International Conference on Correlation Optics, edited
by Oleg V. Angelsky, Proc. of SPIE Vol. 12126, 1212629

7	Reference coherent wave formation block	Polarizing beam splitter
8	Multichannel block for the formation of the polarization structure of the reference coherent wave	Linear ($0^0;90^0;45^0$) and right-circular polarization system (linear polarizer).
10	Discritization block of polarization-interference distribution in the plane of a digital microscopic image	Digital CCD camera (The Imaging Source DMK 41AU02.AS, monochrome 1/2 "CCD, Sony ICX205AL) by polarization microobjective
11	Block for computer processing of polarization interferometry data	Calculation algorithms: - local contrast values at the points of the polarization-interference distribution of the microscopic image.

Fig. 1. Structural and logical diagram of the method of polarization interferometry of microscopic images of histological sections of biopsy of prostate tumours.

2. CHARACTERISTICS OF RESEARCH OBJECTS

The following groups зразків of polycrystalline blood films were studied:

1. Prostate adenoma biopsy control group 1 (36 samples).
2. Highly differentiated adenocarcinoma (3 + 3) of the prostate - study group 2 (36 samples).
3. Medium differentiated adenocarcinoma (3 + 4) of the prostate - study group 3 (36 samples).
4. Low differentiated adenocarcinoma (4 + 4) of the prostate - study group 4 (36 samples).

3. COORDINATE AND STATISTICAL STRUCTURE OF LOCAL CONTRAST MAPS OF MICROSCOPIC IMAGES OF POLYCRYSTALLINE BLOOD FILMS OF PATIENTS OF PROSTATE TUMOURS WITH DIFFERENT DEGREES OF DIFFERENTIATION

Coordinate (fragments (1)) and statistical parameters of histograms (fragments (2)) of the distributions of the magnitude $W(m,n)$ of digital microscopic images of histological sections of biopsy of adenoma and adenocarcinoma with different degrees of differentiation are shown in a series of fragments in Fig. 2 - Fig. 5

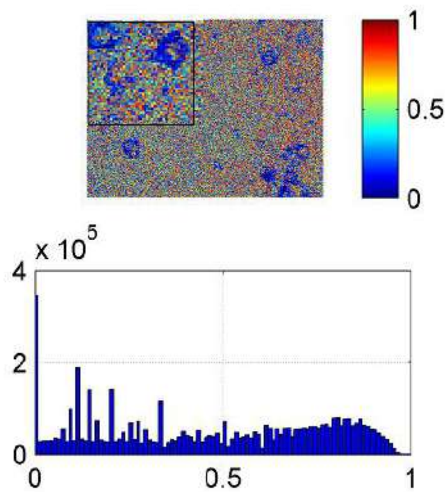

Fig. 2. Map (fragment (1)) and distribution histogram (fragment (2)) of the local contrast value of the polarization-interference microscopic image of the polycrystalline blood film of a patient with adenoma - control group 1.

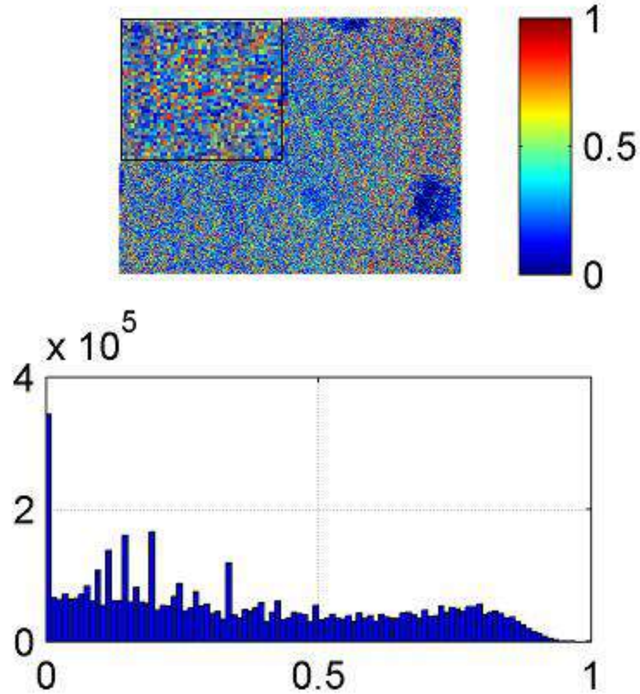

Fig. 3. Map (fragment (1)) and distribution histogram (fragment (2)) of the local contrast value of a polarization-interference microscopic image of a polycrystalline blood film of a patient with adenocarcinoma of high differentiation (3 + 3) - research group 2.

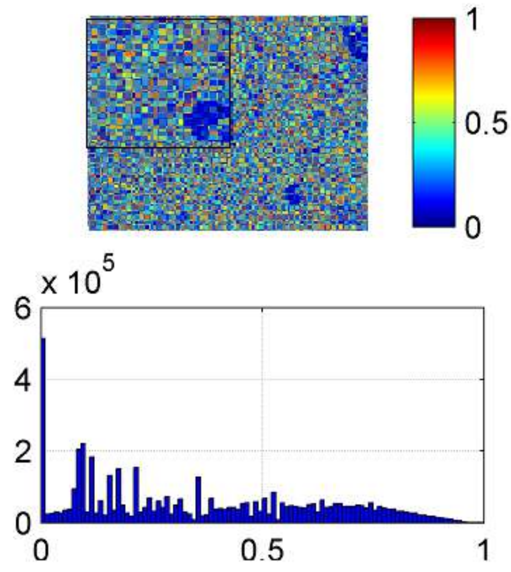

Fig. 4. Map (fragment (1)) and distribution histogram (fragment (2)) of the local contrast value of a polarization-interference microscopic image of a polycrystalline blood film of a patient with adenocarcinoma of medium differentiation (3 + 4) - research group 3.

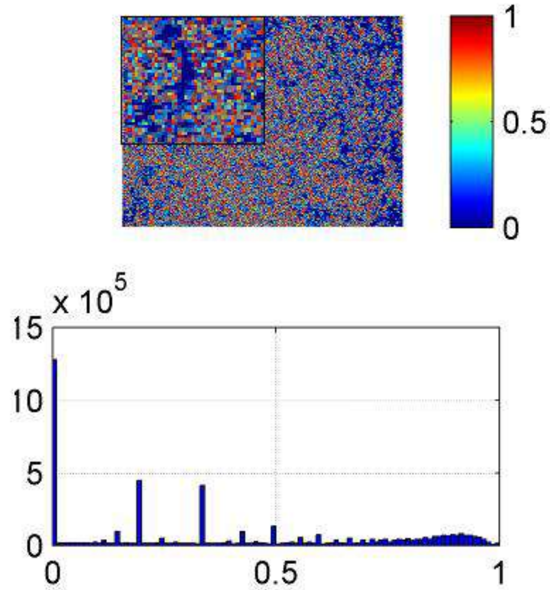

Fig. 5. Map (fragment (1)) and distribution histogram (fragment (2)) of the local contrast value of a polarization-interference microscopic image of a polycrystalline blood film of a patient with adenocarcinoma of low differentiation (4 + 4) - research group 4.

Comparative analysis of the results of polarization-interference measurements of local contrast maps (Fig. 2 - Fig. 5) of digital microscopic images of representative samples of polycrystalline blood film samples from patients in the control (group 1) and all research (group 2 - group 4) groups revealed:

- The presence of the widest possible range of coordinate and quantitative changes in the magnitude of the local contrast of polarization-interference distributions in the plane of digital microscopic images of a set of samples of polycrystalline blood films of patients with adenoma and adenocarcinoma of the prostate of different differentiation according to the Gleason scale – (3+3), (3+4) and (4+4), - $0 \le W \le 1$.

- Individual structure of histograms of distributions of the local contrast value of polarization-interference maps in the plane of digital microscopic images of a set of samples of polycrystalline blood films of patients with adenoma and adenocarcinoma of the prostate of different differentiation according to the Gleason scale – (3+3), (3+4) and (4+4).

- Sequential decrease of the average of histograms of distributions of the local contrast of polarization-interference maps in the plane of digital microscopic images of samples of polycrystalline blood films of patients with adenoma and adenocarcinoma as the degree of differentiation on the Gleason scale decreases – (3+3), (3+4) and (4+4).

This can be associated with biochemical changes in the concentration of blood corpuscles, which lead to a decrease in the level of optical anisotropy in the presence of adenocarcinoma with a decrease in the level of their differentiation. – (3+3), (3+4) and (4+4).

This scenario corresponds to a decrease in phase fluctuations at the points of digital microscopic images of polycrystalline blood films of patients with malignant tumours with low differentiation.

4. STATISTICAL ANALYSIS OF LOCAL CONTRAST MAPS OF DIGITAL MICROSCOPIC IMAGES OF POLYCRYSTALLINE BLOOD FILMS OF PATIENTS WITH PROSTATE TUMOURS OF VARIOUS DIFFERENTIATION

Quantitatively, the scenarios for changing the local contrast maps of microscopic images of polycrystalline blood films are illustrated by a set of mean intragroup values and standard deviations of the magnitude of statistical moments SM_i - Table 1.

Table 1 Statistical parameters of the local contrast map $W(m,n)$ of microscopic images of polycrystalline blood plasma films

Type	Adenoma	Adenocarcinoma (3+3)	Adenocarcinoma (3+4)	Adenocarcinoma (4+4)
SM_1	0.21 ± 0.009	0.14 ± 0.006	0.102 ± 0.005	0.065 ± 0.003
p	$p \leq 0.001$			
		$p \leq 0.05$		
			$p \leq 0.05$	
SM_2	0.29 ± 0.013	0.18 ± 0.08	0.13 ± 0.06	0.09 ± 0.004
p	$p \leq 0.001$			
		$p \leq 0.05$		
			$p \leq 0.05$	
SM_3	0.88 ± 0.038	1.11 ± 0.054	1.46 ± 0.068	1.74 ± 0.079
p	$p \leq 0.001$			
		$p \leq 0.05$		
			$p \leq 0.05$	
SM_4	1.05 ± 0.048	1.44 ± 0.069	1.87 ± 0.088	2.11 ± 0.096
p	$p \leq 0.001$			
		$p \leq 0.05$		
			$p \leq 0.05$	

From the obtained data of the statistical analysis of the local contrast distributions $W(m,n)$, which were determined by the method of polarization-interference mapping of a set of digital microscopic images, the statistical reliability ($p \leq 0.05$ or $p \leq 0.001$) of differentiation of all types of samples of polycrystalline blood films of patients was established.

5. INFORMATIONAL ANALYSIS OF THE DIAGNOSTIC POWER OF THE METHOD OF POLARIZATION-INTERFERENCE MAPPING OF MICROSCOPIC IMAGES OF POLYCRYSTALLINE BLOOD FILMS OF PATIENTS WITH PROSTATE TUMOURS OF VARIOUS DIFFERENTIATION

The following results were obtained:

- Very good level of accuracy of differential diagnosis "adenoma (control group 1) - adenocarcinoma (research group 2 - group 4)" – $Ac = 92\%$;

- Very good level of accuracy of differential diagnosis "adenocarcinoma (3 + 3, - group 2) - adenocarcinoma (4 + 4, - group 4)" – $Ac = 93\% \div 91\%$;
- Good level of accuracy of differential diagnosis "adenocarcinoma (3 + 3, - group 2) - adenocarcinoma (3 + 4, - group 3)" – $Ac = 88\%$;
- Satisfactory level of accuracy of differential diagnosis "adenocarcinoma (3 + 4, - group 3) - adenocarcinoma (4 + 4, - group 4)" – $Ac = 84\%$.

CONCLUSIONS

1. The possibilities of the polarization-interference approach to the analysis of microscopic images of polycrystalline blood films in the differential diagnosis of benign and malignant tumours of the prostate with varying degrees of differentiation have been experimentally investigated and clinically analyzed.

2. A complex cycle of measuring and analyzing the topographic structure of maps and histograms of the distribution of the local contrast value of polarization-interference distributions of digital microscopic images of a set of representative samples of samples of polycrystalline blood films of patients in the control and experimental groups has been implemented.

3. Statistical criteria for polarization-interference diagnostics of a set of representative samples of samples of polycrystalline blood films of patients from the control and experimental groups have been established and analytically substantiated..

4. As part of the information analysis, the operational characteristics (sensitivity, specificity, accuracy) of the diagnostic strength of the polarization interferometry method for differential diagnosis of polycrystalline blood films of patients from the control and experimental groups were determined.

FUNDING

Current research supported by the National Research Foundation of Ukraine (Project 2020.02/0061)

REFERENCES

[1] V. Shankaran, J. T. Walsh, Jr., and D. J. Maitland, "Comparative study of polarized light propagation in biological tissues," J. Biomed. Opt. 7(3), 300–306 (2002).
[2] I. M. Stockford et al., "Analysis of the spatial distribution of polarized light backscattering," J. Biomed. Opt. 7(3), 313–320 (2002).
[3] X. Wang and L. V. Wang, "Propagation of polarized light in birefringent turbid media: a Monte Carlo study," J. Biomed. Opt. 7(3), 279–290 (2002).
[4] K. C. Hadley and I. A. Vitkin, "Optical rotation and linear and circular depolarization rates in diffusively scattered light from chiral, racemic, and achiral turbid media," J. Biomed. Opt. 7(3), 291–299 (2002).
[5] V. V. Tuchin, L. Wang, and D. A. Zimnyakov, Optical Polarization in Biomedical Applications, Springer, New York (2006).
[6] A. De Martino, Ed., "A polarization-based optical techniques applied to biology and medicine," in Proc. European Workshop, Ecole Polytechnique, Massy, France (2009).
[7] G. L. Coté and B. D. Cameron, "A noninvasive glucose sensor based on polarimetric measurements through the aqueous humor of the eye," in Handbook of Optical Sensing of Glucose in Biological Fluids and Tissues, V. V. Tuchin, Ed., pp. 183–211, CRC Press, Taylor & Francis Group, London (2009).
[8] Ushenko, V.O., Trifonyuk, L., Ushenko, Y.A., Dubolazov, O.V., Gorsky, M.P., Ushenko, A.G. Polarization singularity analysis of Mueller-matrix invariants of optical anisotropy of biological tissues samples in cancer diagnostics (2021) Journal of Optics (United Kingdom), 23 (6), 064004.

[9] Meglinski, I., Trifonyuk, L., Bachinsky, V., Vanchulyak, O., Bodnar, B., Sidor, M., Dubolazov, O., Ushenko, A., Ushenko, Y., Soltys, I.V., Bykov, A., Hogan, B., Novikova, T. Polarization Correlometry of Microscopic Images of Polycrystalline Networks Biological Layer (2021) SpringerBriefs in Applied Sciences and Technology, pp. 61-73.

[10] Meglinski, I., Trifonyuk, L., Bachinsky, V., Vanchulyak, O., Bodnar, B., Sidor, M., Dubolazov, O., Ushenko, A., Ushenko, Y., Soltys, I.V., Bykov, A., Hogan, B., Novikova, T. Scale-Selective and Spatial-Frequency Correlometry of Polarization-Inhomogeneous Field (2021) SpringerBriefs in Applied Sciences and Technology, pp. 33-59.

[11] Angelsky, O.V., Bekshaev, A.Y., Hanson, S.G., Zenkova, C.Y., Mokhun, I.I., Jun, Z. Structured Light: Ideas and Concepts (2020) Frontiers in Physics, 8, 114

[12] Angelsky, O.V., Ushenko, Y.A., Dubolazov, A.V., Telenha, O.Yu. The interconnection between the coordinate distribution of mueller-matrixes images characteristic values of biological liquid crystals net and the pathological changes of human tissues (2010) Advances in Optical Technologies, 130659

[13] Meglinski, I., Trifonyuk, L., Bachinsky, V., Vanchulyak, O., Bodnar, B., Sidor, M., Dubolazov, O., Ushenko, A., Ushenko, Y., Soltys, I.V., Bykov, A., Hogan, B., Novikova, T. Methods and Means of Polarization Correlation of Fields of Laser Radiation Scattered by Biological Tissues (2021) SpringerBriefs in Applied Sciences and Technology, pp. 1-15.

[14] Meglinski, I., Trifonyuk, L., Bachinsky, V., Vanchulyak, O., Bodnar, B., Sidor, M., Dubolazov, O., Ushenko, A., Ushenko, Y., Soltys, I.V., Bykov, A., Hogan, B., Novikova, T. Materials and Methods (2021) SpringerBriefs in Applied Sciences and Technology, pp. 17-31.

[15] Trifonyuk, L., Sdobnov, A., Baranowski, W., Ushenko, V., Olar, O., Dubolazov, A., Pidkamin, L., Sidor, M., Vanchuliak, O., Motrich, A., Gorsky, M., Meglinski, I Differential Mueller matrix imaging of partially depolarizing optically anisotropic biological tissues (2020) Lasers in Medical Science, 35 (4), pp. 877-891.

[16] Angelsky, O.V., Bekshaev, A.Y., Dragan, G.S., Maksimyak, P.P., Zenkova, C.Y., Zheng, J. Structured Light Control and Diagnostics Using Optical Crystals (2021) Frontiers in Physics, 9,715045.

[17] Angelsky, O.V., Maksimyak, P.P. Optical diagnostics of slightly rough surfaces (1992) Applied Optics, 31 (1), pp. 140-143

[18] Angelsky, O.V., Zenkova, C.Y., Hanson, S.G., Zheng, J. Extraordinary Manifestation of Evanescent Wave in Biomedical Application (2020) Frontiers in Physics, 8, 159.

[19] Angelsky, O.V., Hanson, S.G., Maksimyak, A.P., Maksimyak, P.P. On the feasibility for determining the amplitude zeroes in polychromatic fields (2005) Optics Express, 13 (12), pp. 4396-4405

[20] Borovkova, M., Trifonyuk, L., Ushenko, V., Dubolazov, O., Vanchulyak, O., Bodnar, G., Ushenko, Y., Olar, O., Ushenko, O., Sakhnovskiy, M., Bykov, A., Meglinski, I. Mueller-matrix-based polarization imaging and quantitative assessment of optically anisotropic polycrystalline networks (2019) PLoS ONE, 14 (5), e0214494 .